Available online at www.sciencedirect.com

ScienceDirect

Energy Procedia 148 (2018) 344–351

Energy Procedia

www.elsevier.com/locate/procedia

73rd Conference of the Italian Thermal Machines Engineering Association, ATI2018, 12-14 September 2018, Pisa, Italy

Reduction of the experimental effort in engine calibration by using neural networks and 1D engine simulation

Francesco de Nola[a], Giovanni Giardiello[b]*, Alfredo Gimelli[b], Andrea Molteni[a], Massimiliano Muccillo[b], Roberto Picariello[a], Diego Tornese[a].

[a]*Teoresi S.p.A. – via F. Imparato 198, 80146 Napoli, Italy*
[b]*Università degli Studi di Napoli Federico II - Corso Umberto I 40 - 80138 Napoli, Italy*

Abstract

In this study, two effective methodologies are proposed to overcome some critical issues concerning the base calibration of engine control parameters. Specifically, Neural Networks and 1D CFD simulation were alternatively adopted to reliably calibrate specific ECU functions starting from a reduced number of experimental data. The calibration performance fall within acceptable limits even when significant cuts are made to the experimental data usually acquired for calibration purposes, demonstrating that the proposed methodologies can be useful to significantly reduce the dynamometer tests and their related times and costs.

Keywords: Engine Electronic Control Unit; Engine management system; Computer aided calibration; Neural Networks; 1D engine simulation

1. Introduction

Over the last decades, the automotive industry had to cope with severe challenges that have driven the evolution of reciprocating internal combustion engines. In particular, subsequent EU regulations set increasingly stringent emission standards [1] and, more recently, average CO_2 emission limits for new passenger cars. The achievement of these often-

* Corresponding author. Tel.: +393311112468.
E-mail address: Giovanni.giardiello@unina.it

10.1016/j.egypro.2018.08.087

conflicting goals led to the development of complex engine architectures needed to perform advanced management strategies [2]. Therefore, Variable Valve Actuation, Exhaust Gas Recirculation [3], Gasoline Direct Injection, and other technologies have largely equipped modern internal combustion engines. However, such complex engines provide a large set of degrees of freedom available for the engine regulation, introducing many new control variables within the control systems and resulting in a very expensive and long calibration process.
To mitigate these criticalities, this study proposes the adoption of two effective methodologies based on the use of artificial Neural Networks (NN) [4]-[6] and 1D CFD simulation. Specifically, NN and 1D CFD are respectively used to generate mathematical and physical models of the engine behavior starting from a small subset of the engine operating conditions usually tested for calibration purposes. Therefore, detailed engine data sheets are provided starting from a reduced number of experimental data.

Nomenclature

$PRES$	value of the manifold pressure
C_{PRES}	correction coefficient that takes account of the pressure drop through the valves
V_{EFF}	air volume actually available for the combustion process
V_{EGR}	value of the mass of exhaust gas trapped in the cylinder
M_{AIR}	air mass trapped within the engine cylinder
R	universal gas constant
T_{AIR}	air temperature
VOL_{EFF}	volumetric efficiency evaluated by the ECU
VOL_{EFF_TB}	volumetric efficiency evaluated at bench test
M_{REF}	theoretical trapped air mass in the cylinder
VVT	angle of valve closing
RPM	engine speed
$err\%$	percentage error of the volumetric efficiency
T	initial training set
ω_j	neural networks weights
h_j	basis function
H	matrix of all the RBF
RBF	radial basis function
NN	neural network
ρ_u	density of the mixture
C	calibration parameter
A_L	surface of discontinuity between burned and unburned gases
S_T	flame turbulent speed
S_L	flame laminar speed
m_e	encapsulated mass
m_b	burned mass
τ	chemical reaction time
λ	front thickness
c_{dw}	valve discharge coefficient
$A_{ref,v}$	valve reference area
P	pressure
$\dot{Q}_w$	thermal power
h_w	coefficient of conductive heat exchange

2. Improving the calibration process: the proposed methodologies

As previously said, the EECU is fundamental to control the engine operation. It receives input signals from on-board sensors and other control units; the signals are then processed through a series of logical operations before the EECU returns signals as output, which will be used by other control units or actuators. The engine control unit includes several functions which provide simplified models of more complex physical phenomena. These functions use map, scalar and/or vector calibration parameters to process input signals related to the current operating condition of the vehicle and estimate a physical quantity that is returned as output. The base calibration is intended to identify proper values for the calibration parameters so that the values estimated by the functions are as close as possible to those that can be measured at the test bench in the same operating condition for the same quantity.
Fig 1, on the left, shows the main stages of a conventional calibration process. Usually, an experimental campaign is carried out according to specific and predefined engine operating strategies. Therefore, all the physical quantities needed for the calibration of the EECU functions are acquired and recorded in a datasheet. The calibration process is mathematically assisted through dedicated software aimed at error minimization and maps optimization. Finally, in the fourth phase, the accuracy of the calibration process is verified at the test bench. This process can be cyclically repeated until the difference between the output values provided by the calibrated ECU are reasonably close to those which were measured during the experimental campaign.

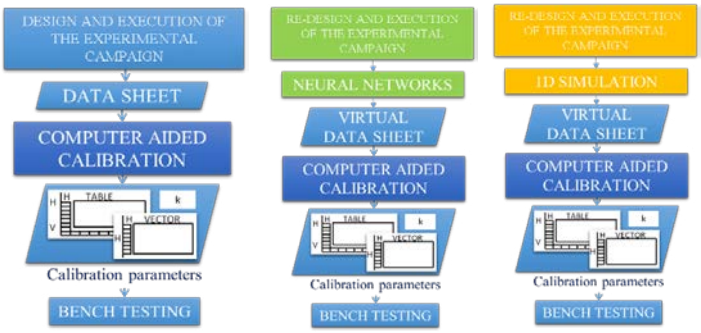

Fig 1 - Main stages of the conventional calibration process (on the left), and the proposed processes (in the middle and on the right).

The experimental activity, which can last several weeks, is the most critical stage of the process in terms of time and cost of implementation. Moreover, as the powertrain complexity increases, the calibration effort grows exponentially so that the achievement of optimized calibrations may be theoretically impossible without the use of advanced Computer Aided Calibration procedures. In addition, the system complexity featured by current engines requires a further increase in experimental tests needed to achieve a reliable calibration.
To overcome this criticality, this study proposes the adoption of two alternative methodologies based on the use of Neural Networks and 1D CFD simulation. Specifically, NN and 0D-1D thermo-fluid dynamic simulation are respectively used to generate mathematical and physical models of the engine behavior starting from a small subset of the engine operating conditions usually tested for calibration purposes. In particular, 0D-1D CFD simulation codes, after being reliably calibrated, could be useful to greatly reduce dynamometer tests of advanced powertrains from thousands of operating conditions to a few tens.

3. The volumetric efficiency function and its reference calibration performance

All the results discussed in this research work refer to a two-cylinder turbocharged engine equipped by a fully flexible electro-hydraulic valve actuation system for the intake valves (Table 1).

Table 1 – Engine main characteristics.

Model	Turbocharged, 2 cylinders, 8 valves, VVA
Displacement	875 cm^3
Stroke/Bore	86 mm / 80.5 mm
Connecting Rod Length	136.85 mm
Compression Ratio	9.9

Moreover, in this paper, the proposed methodologies have been applied to the base calibration of the volumetric efficiency function as implemented in the ECU of the reference engine. To assess the effectiveness of these methodologies, a complete set of data usually adopted for the base calibration of the volumetric efficiency function is adopted while the calibration performance is evaluated by mean of a specific Computer Aided Calibration algorithm developed by the authors and whose details are discussed in [7]. The experimental campaign includes data concerning 680 engine operating conditions. The volumetric efficiency is a fundamental engine quantity which is not directly measurable from the sensors available on marketed vehicles. It is used to evaluate the engine torque, to set the spark advance and the throttle position. Based on the ideal gas law equation, this estimation function is implemented in the engine control unit under investigation in the following form:

$$(PRES \cdot C_{PRES}) \cdot V_{EFF} = M_{AIR} \cdot R \cdot T_{AIR} - V_{EGR} \cdot PRESS_{EX} \quad (1)$$

where $PRES$ is the value of the manifold pressure, corrected by C_{PRES} that is a correction coefficient that takes account of the pressure drop through the valves; V_{EFF} represents the air volume actually available for the combustion

process, R is the specific gas constant, T_{AIR} is the air temperature, V_{EGR} is the mass of exhaust gas which at the end of the exhaust valve closing remains trapped in the cylinder, $PRESS_{EX}$ is the pressure of the exhaust gas and M_{AIR} is the unknown air mass trapped within the engine cylinder. The volumetric efficiency is given by the ratio of M_{AIR} to M_{REF}, which represents the theoretical air mass trapped in the cylinder in ambient conditions:

$$VOL_{EFF} = \frac{M_{AIR}}{M_{REF}} \qquad (2)$$

Therefore, to reliably estimate the volumetric efficiency in all the engine operating conditions, three parameters represented by lookup tables must be calibrated. These parameters depend on manifold pressure, engine speed and variable valve timing angle as follows:

- $C_{PRES} = f(VVT, PRESS)$;
- $V_{EFF} = f(VVT, RPM)$;
- $V_{EGR} = f(VVT, RPM)$.

Starting from a datasheet consisting of 680 rows representing the 680 engine operating conditions previously measured at the test bench, the calibration software extracts these three quantities (*RPM*, *PRES*, *VVT*), together with the volumetric efficiency, from the available set of data. Then, the estimation of the volumetric efficiency is performed by using the equations (1) and (2). Finally, the calibration performance is evaluated by comparing the errors between estimated and measured values of the volumetric efficiency at each operating condition:

$$err\% = \frac{VOL_{EFF} - VOL_{EFF\_TB}}{VOL_{EFF\_TB}} \cdot 100 \qquad (3)$$

Where VOL_{EFF_TB} is the volumetric efficiency evaluated at the test bench. The percentage error distribution is represented in a diagram highlighting the rate of the calculated errors that falls within the acceptable limits established by the engine manufacturer. Fig 2 compares the error distribution for the volumetric efficiency when an uncalibrated ECU function is used (i.e. C_{PRES}, V_{EFF} and V_{EGR} are calculated using default values of the lookup tables), on the left, to the distribution obtained for the calibrated function. In the first case, only the 22% of the errors falls within the fixed acceptable limit of 5% represented by the red lines. In the second case, the 95.44% of the errors fall within the acceptable range. This value has been used as a reference calibration performance to assess the potential of the proposed methodologies.

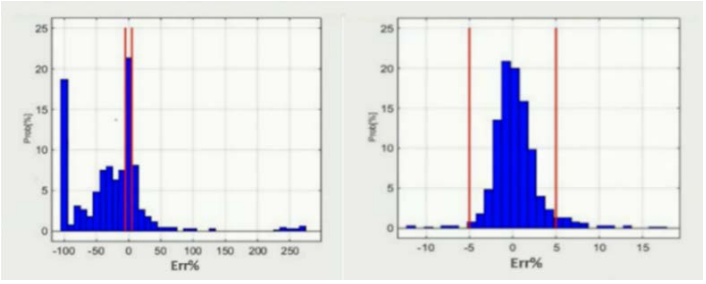

Fig 2. Error distributions for the uncalibrated (on the left) and the calibrated volumetric efficiency function (on the right).

4. The use of Neural Networks to reduce the experimental effort in engine base calibration

The first proposed methodology is based on the adoption of radial basis function networks. A neural network is an example of response surface methodology (RSM). RSM is a collection of mathematical and statistical techniques that are used in engineering design to define approximations of analysis codes. A NN is based on an initial training set of data indicated as follows:

$T = (x_i, \hat{y}_i)$ where $i = 1, \ldots, n$ (4)

The symbol adopted for $\hat{y}_i$ indicates that the value of the response variable is not exactly determined, as it may be affected by dispersion or by measurement errors. The function in question can be expressed as a linear combination of a set of m other functions $h(x)$, called basis functions, and parameters ω, called weights, according to the following formulation:

$f(x) = \sum_{j=1}^{m} \omega_j h_j(x)$ (5)

A radial basis function network is an artificial neural network that uses radial basis functions (RBF) [8]-[9] as activation functions. These functions can be monotonically increasing or decreasing with their values depending on

the distance from a fixed point called center. An RBF neural network is obtained, therefore, by using these particular functions in equation (5), where they act as activation functions. As shown in Fig 3, the resulting NN consists of three layers: an input layer, in green, directly connected to the training set; a hidden layer, in orange, where the neurons are located and non-linear transformations take place by means of RBF; an output layer, in blue. The RBFs that act as activation function in the neurons of the hidden layer are characterized by centroids that are selected among the input data. These centers constitute the nodes of the hidden layer and each of the samples of the input set feeds these nodes. The resulting function $f(x)$ is therefore the approximand of a series of *m d*-dimensional non-linear functions provided as output of the output layer, namely:

$$f(x) = \sum_{i=1}^{m} \omega_i h_i(x)(\|x - c_i\|) = H\omega \qquad (6)$$

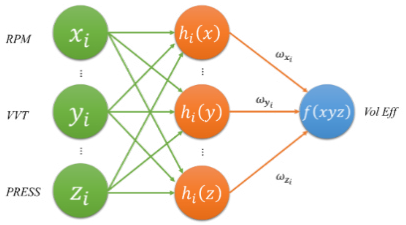

Fig 3. Structure of a neural network with specification of the ECU engine quantities adopted within the input and output layers.

where:

- ω_i are the weights belonging to the vector ω that must be determined by imposing that the distance between the final predictive model and the RBF tends to zero;
- $\|x - c_i\|$ is the Euclidean distance between a centroid and the points of the input set;
- *H*, called interpolation matrix, is the matrix of all the RBF;
- *m*, apart from representing the number of RBF, is also the number of hidden layer neurons. Each of these neurons acts in a localized region of space on the assigned input data; the activation of these neurons is determined by the distance between the input vector and the response predictive vector.

In this paragraph, a NN is used to reduce the experimental effort required for the calibration of the volumetric efficiency function implemented into the ECU of the reference internal combustion engine. To this aim, starting from the experimental datasheet usually used for the calibration of the volumetric efficiency function and previously adopted to achieve the results represented in Fig 2, an increasing number of rows, which represents the number of measured engine operating conditions, has been randomly deleted from the available set of data. The reduced datasheet is used to train the neural network whose structure is represented in Fig 3. In this way, the neural network is used to estimate the volumetric efficiency in the operating conditions whose experimental data were previously deleted. Finally, the reconstructed data sheet is used for the calibration of the ECU function under investigation. Eventually, the calibration performance achieved is compared to the reference calibration obtained through the application of the calibration process to the original data sheet (right side of Fig 2). In Fig 3, the input layer, x_i represents the parameter *RPM*, y_i the values of *PRES* and z_i the values of *VVT*, while the volumetric efficiency was set as dependent variable and its values are obtained as output. The neural network defines a functional relationship between the input and the output, providing estimation values for the volumetric efficiency in the operating conditions previously deleted. Therefore, a mixed experimental-numerical datasheet (here called virtual datasheet) consisting of 680 operating conditions, which includes the same operating conditions previously deleted, can be generated. To validate the proposed methodology, the virtual datasheet is used as input to the calibration software as represented in the scheme in the middle of Fig 1. The volumetric efficiency function is then calibrated and the calibration performance compared with that obtained through the complete experimental datasheet. The results achieved with a random reduction of 40, 50 and 60% of the experimental values for the volumetric efficiency are shown in Fig 4. In particular, the percentage occurrence for the calibration obtained with a reduction of the 40% of the original datasheet is shown on the left. The acceptable range of ± 5% is also highlighted. In this case, 94,71% of the values falls within the acceptable range, meaning that a calibration performance that is very close to the reference case shown in Fig 2 can be obtained despite a 40% cut to the experimental acquisitions.

To verify the potential of the proposed methodology, further calibration processes have been performed after randomly

cutting the original experimental data set by 50% (in the middle of Fig 4) and 60% (right side of Fig 4) respectively, and 60%. Results show no significant degradation of calibration performance even if a 60% reduction of the original data set is considered. In fact, in the first case the 94.26% of the values falls within the acceptable range. A slightly lower percentage of 93.68% falls within the acceptable range even if a 60% reduction of the data set is accepted, showing a calibration performance reduction of approximately 2% if compared to the result achievable using the original data from dynameter tests.

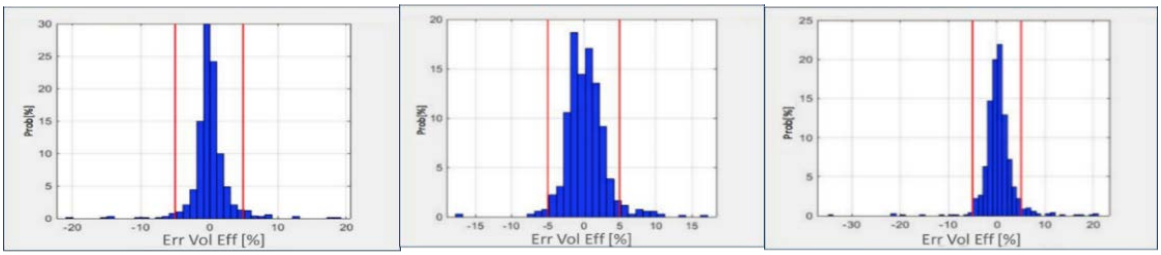

Fig 4. Error distributions achieved by using NN recalculation for the volumetric efficiency function: 40% reduction (on the left), 50% reduction (in the middle) and 60% reduction (on the right) of the original data set.

5. The use of 1D thermo-fluid dynamic simulation to reduce the experimental effort in engine base calibration

Starting from a small subset of data selected from a datasheet including 528 operating condition of the reference twin cylinder downsized engine, a 0D-1D CFD model of the spark ignited engine has been set and then calibrated by using an evolutionary genetic algorithm and the vector optimization approach [10-14]. The experimental campaign has been performed according to particular engine operating strategies used for EECU calibration purposes which will be described in this paragraph. As for the optimization problem, specific calibration constants have been set as decision variables within the multi-objective optimization process while the error minimization between calculated and measured relevant engine quantities have been imposed as objective functions of the problem. The error minimization has been pursued with reference to several operating conditions of the engine. Specifically, this work focuses on three calibration constants ($\boldsymbol{C_1}, \boldsymbol{C_2}, \boldsymbol{C_3}$) related to the combustion process, which is modelled through the following two equations addressing the mass entrainment rate into the flame front and the burn rate [15]-[17]:

$$\left(\frac{dm_e}{dt}\right) = \rho_u \boldsymbol{C_1} A_L (\boldsymbol{C_2} S_T + S_L) \quad (7)$$

Where m_e is the entrained mass of unburned, ρ_u is the density of the air-fuel mixture, A_L is the entrainment surface of the flame front, S_T and S_L are the turbulent and laminar flame speed, respectively. The burn rate is then:

$$\left(\frac{dm_b}{dt}\right) = \frac{m_e - m_b}{\boldsymbol{C_3}\tau} \quad (8)$$

Where, m_b is the burned mass, τ is a time constant calculated as follows: $\tau = \frac{\lambda}{S_L}$, where λ and S_L are respectively the Taylor microscale length and the laminar flame speed. A further calibration constant, $\boldsymbol{C_4}$, is used as follows to reliably estimate the pressure drop through the valves:

$$\frac{dm}{dt} = \boldsymbol{C_4}\, c_{dw} A_{ref,v} p_1 \sqrt{\frac{2\gamma}{\gamma-1}\frac{1}{RT_1}\left[\left(\frac{p_2}{p_1}\right)^{2/\gamma} - \left(\frac{p_2}{p_1}\right)^{\gamma+1/\gamma}\right]} \quad (9)$$

Finally, a last calibration constant is related to heat exchange through the cylinder walls according to the following equation:

$$\dot{Q}_w = \boldsymbol{C_5} h_w A_w (T - T_w) \quad (10)$$

Aa already said, the objective functions have been defined as the differences between experimental and numerical values of specific engine quantities. In particular, the errors refer to the following quantities: brake torque, break specific fuel consumption, air mass flow rate, turbocharger rotational speed, maximum cylinder pressure and crank angular position at maximum pressure. Moreover, the error minimization has been pursued with reference to 16 different operating conditions of the engine. Therefore, the optimization problem is defined by 5 decision variables and 96 objective functions. Among the solutions belonging to the Pareto optimal front, the one that minimizes the total average error was selected and the average errors achieved are summarized in Table 2. Table 2 also shows a

comparison with the errors achieved for the same quantities by mean of a heuristic calibration, highlighting how the average error falls from 5.44% to 3.31%. After calibrating the engine model, two virtual dynamometer tests have been the execution to derive the virtual datasheets that will be used, in a future work, as input to the calibration software according to the flowchart reported on the right side of Fig 1.

Table 2. Average percentage errors for some relevant engine quantities: heuristic vs calibration achieved through vector optimization.

	Torque	BSFC	Air mass flow	Turbine Speed	Pmax	Ang_Pmax	Average Error
	7,06	6,39	3,05	3,27	5,44	7,44	5,44
5x96	2,64	3,39	3,24	3,51	4,25	2,77	3,31

The implemented strategies faithfully reproduce those adopted during the experimental campaigns for which experimental data are available, here named Strategy 1 and Strategy 2. Strategy 1, in turn, includes two different phases, namely Phase 1 and Phase 2. In Phase 1, the engine speed increases by steps (i.e. 1500, 1800, 2000… 5500 rpm, as you can see below), the intake valves perform the maximum lift and the wastegate is completely open. For each operating condition (i.e. for each engine speed), the throttle valve opening sweeps from the minimum allowable pressure to WOT and the spark advance is set to reach the maximum torque or incipient detonation.
In Phase 2, the engine speed is varied as in Phase 1, the throttle valve is completely open and the intake valves perform the maximum lift. For each operating condition (or engine speed) the wastegate opening is changed in order to obtain sweeps by 200 mbar at a time of the boost pressure until its maximum allowable value is reached. The spark advance is regulated to reach maximum torque or incipient detonation.
In the Strategy 2, the engine speed increases by fixed steps while the wastegate is completely opened. For each operating condition, the intake valves closing angle (i.e. EIVC) sweeps from the minimum to the maximum value, the spark advance is regulated to reach maximum torque or incipient detonation and the throttle valve is regulated to reach a downstream/upstream pressure ratio of 0.88. These virtual dynamometer tests were carried out under different engine speeds: 5500, 5100, 4800, 4400, 4000, 3600, 3300, 3000, 2700, 2500, 2300, 2000, 1800, 1500 RPM. At each engine speed, all the physical quantities needed for the calibration process were calculated and the virtual datasheet was obtained. The Strategy 1 leads to simulate 160 engine operating conditions for the Phase 1 and 83 for the Phase 2. The Strategy 2 involves 285 operating conditions. To verify the effectiveness of the proposed methodology, both the virtual datasheets were compared with the related experimental data. The results are shown in Fig 5.

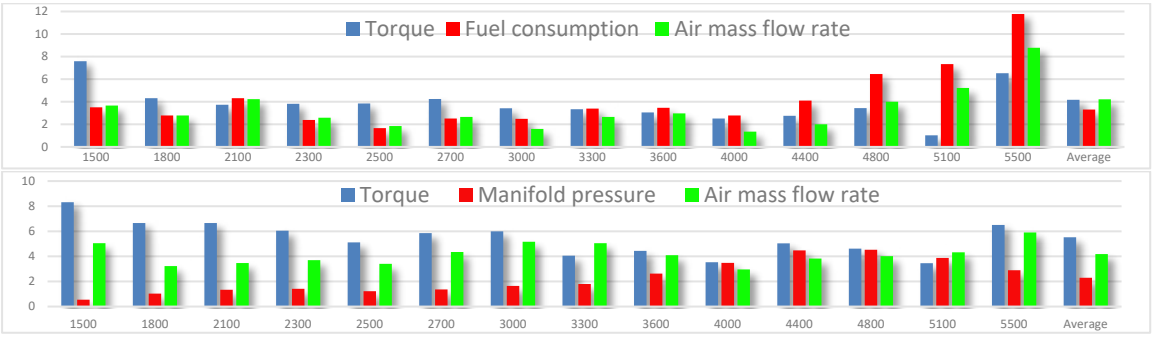

Fig 5. Average errors between experimental and numerical values: Strategy 1 (at the top) and Strategy 2 (below).

In particular, as for the Strategy 1, the errors refer to the engine torque, the specific fuel consumption and the air mass flow rate. Each bar in the figure represents the average percentage errors at each engine speed. It can be noted that this error varies between 1.02% to 11.77%. As for the Strategy 2, reference is made to the engine torque, the manifold pressure and the air mass flow rate (the graph below in Fig 5). In this case, the average error varies between 8.05% for the manifold pressure at 1500 RPM and 0.35% of for the torque at 1500 RPM. However, the average error remains relatively low. With the second acquisition strategy, for example, the average error varies between 5.52% for the torque to 2.30% for the manifold pressure. These values could be comparable with the measurement errors, demonstrating the effectiveness of the proposed methodology.

6. Conclusion

In this study, two effective methodologies are proposed to overcome some critical issues concerning the base calibration of engine control parameters. Specifically, Neural Networks and 1D CFD simulation were alternatively adopted to reliably calibrate specific ECU functions starting from a reduced number of experimental data. The first methodology provides calibration performance falling within acceptable limits even when significant cuts are made to the experimental data usually acquired for calibration purposes, demonstrating that the proposed methodologies can be useful to significantly reduce the dynamometer tests and their related times and costs.

The second methodology also shows promising results, as the average errors could be comparable with the measurement errors, demonstrating the effectiveness of the proposed methodology. Therefore, future works will address the use of the numerical data obtained from the proposed methodology based on 1D CFD analysis as input to the calibration software. In this way, the calibration of specific EECU functions could be performed according to the flowchart represented in Fig 1.

References

[1] Napolitano P. et al, "Study of the Effect of the Engine Parameters Calibration to Optimize the Use of Bio-Ethanol/RME/Diesel Blend in a Euro5 Light Duty Diesel Engine", SAE International Journal of Fuels and Lubricants, Volume 6, Issue 1, April 2013, Pages 263-275.

[2] De Bellis V. et al., Effects of Pre-Lift Intake Valve Strategies on the Performance of a DISI VVA Turbocharged Engine at Part and Full Load Operation, Energy Procedia, Volume 81, December 2015, Pages 874-882. ELSEVIER. ISSN: 1876-6102. doi:10.1016/j.egypro.2015.12.141.

[3] Beatrice C. et al, "Emission reduction technologies for the future low emission rail diesel engines: EGR vs SCR", SAE Technical Papers, Volume 6, 2013, 11th International Conference on Engines and Vehicles, ICE 2013; Capri, Naples; Italy; 15 September 2013 through 19 September 2013; Code 100868.

[4] Lowe D. et al., Validation of Neural Networks in Automotive Engine Calibration. Artifical Neural Networks, 7-9 July 1997, Conference Publication No. 440, IEE.

[5] Yu-Jia Zhai, Ding-Li Yu, Neural network model-based automotive engine air/fuel ratio control and robustness evaluation, Engineering Applications of Artificial Intelligence 22 (2009) 171-180.

[6] P.J. Shayler et al., The exploitation of neural networks in automotive engine management systems, Engineering Applications of Artificial Intelligence, Volume 13, Issue 2, 1 April 2000, Pages 147-157.

[7] de Nola, F., Giardiello, G., Gimelli, A., Molteni, A. et al., "A Model-Based Computer Aided Calibration Methodology Enhancing Accuracy, Time and Experimental Effort Savings Through Regression Techniques and Neural Networks", SAE Technical Paper 2017-24-0054, 2017, https://doi.org/10.4271/2017-24-0054.

[8] M. D. Buhmann, Radial basis functions, Acta numerica, 2000, Acta Numer., vol. 9, Cambridge Univ. Press, Cambridge, 2000, pp. 1-38.

[9] M. D. Buhmann, Radial basis functions, Cambridge Monographs on Applied and Computational Mathematics, vol. 12, Cambridge University Press, Cambridge, 2003.

[10] Coello CA, Van Veldhuizen DA, Lamont GB. Evolutionary algorithms for solving multi-objective problems. Springer US; 2007. http://dx.doi.org/10.1007/978-0-387-36797-2.

[11] Lotov AV, Bushenkov VA, Kamenev GK. Interactive decision maps: approximation and visualization of Pareto Frontier. Boston: Kluwer Academic Publishers; 2004.

[12] Branke J, Deb K, Miettinen K., Slowinski R., Multiobjective Optimization. Interactive and Evolutionary Approaches, 2008. Springer. ISBN 978-3-540-88908-3. DOI: 10.1007/978-3-540-88908-3.

[13] Carlo Poloni, Andrea Giurgevich, Luka Onesti, Valentino Pediroda. Hybridization of a multi-objective genetic algorithm, a neural network and a classical optimizer for a complex design problem in fluid dynamics. Comput. Methods Appl. Mech. Engrg. 186 (2000) 403-420.

[14] C. Poloni, V. Pediroda. GA coupled with computationally expensive simulations: tools to improve efficiency. Genetic Algorithms and Evolution Strategies in Engineering and Computer Science, pages 267-288, John Wiley and Sons, England, 1997.

[15] Hires, S.D., Tabaczynski, R.J., and Novak, J.M., "The Prediction of Ignition Delay and Combustion Intervals for a Homogeneous Charge, Spark Ignition Engine," SAE Paper 780232.

[16] Blizard, N.C. and Keck, J.C., "Experimental and Theoretical Investigation of Turbulent Burning Model for Internal Combustion Engine," SAE Paper 740191, 1974.

[17] Morel, T., Rackmil, C.I., Keribar, R., and Jennings, M.J., "Model for Heat Transfer and Combustion in Spark-Ignited Engine and Its Comparison with Experiments," SAE 880198, 1988.